Proceedings of the ASME 2013 International Design Engineering Technical Conferences &
Computers and Information in Engineering Conference
IDETC/CIE 2013
August 4-7, 2013, Portland, Oregon

DETC2013-12088

ASSURED SAFETY DRILL WITH BI-STABLE BIT RETRACTION MECHANISM

Paul M. Loschak
Harvard School of Engineering and Applied Sciences
Cambridge, MA, USA

Kechao Xiao
Harvard School of Engineering and Applied Sciences
Cambridge, MA, USA

Hao Pei
Harvard School of Engineering and Applied Sciences
Cambridge, MA, USA

Samuel B. Kesner, PhD
Wyss Institute for Biologically Inspired Engineering
Harvard School of Engineering and Applied Sciences
Cambridge, MA, USA

Ajith J. Thomas, MD
Division of Neurosurgery
Beth Israel Deaconess Medical Center
Boston, MA, USA

Conor J. Walsh, PhD
Wyss Institute for Biologically Inspired Engineering
Harvard School of Engineering and Applied Sciences
Cambridge, MA, USA

ABSTRACT

A handheld, portable cranial drilling tool for safely creating holes in the skull without damaging brain tissue is presented. Such a device is essential for neurosurgeons and mid-level practitioners treating patients with traumatic brain injury. A typical procedure creates a small hole for inserting sensors to monitor intra-cranial pressure measurements and/or removing excess fluid. Drilling holes in emergency settings with existing tools is difficult and dangerous due to the risk of a drill bit unintentionally plunging into brain tissue. Cranial perforators, which counter-bore holes and automatically stop upon skull penetration, do exist but are limited to large diameter hole size and an operating room environment. The tool presented here is compatible with a large range of bit diameters and provides safe, reliable access. This is accomplished through a dynamic bi-stable linkage that supports drilling when force is applied against the skull but retracts upon penetration when the reaction force is diminished. Retraction is achieved when centrifugal forces from rotating masses overpower the axial forces, thus changing the state of the bi-stable mechanism. Initial testing on ex-vivo animal structures has demonstrated that the device can withdraw the drill bit in sufficient time to eliminate the risk of soft tissue damage. Ease of use and portability of the device will enable its use in unregulated environments such as hospital emergency rooms and emergency disaster relief areas.

INTRODUCTION

Gaining access to the inside of the skull is an important step for diagnosing and treating many traumatic head injuries. Head trauma can cause traumatic brain injury (TBI) and a number of negative side effects such as swelling of brain tissue, blood hemorrhaging, or cerebrospinal fluid buildup. All of these effects can result in a large increase in pressure inside the cranial cavity. This pressure increase can even cause herniation, which is a potentially fatal condition where pressure build-up forces brain tissue into different sections of the skull, such as through the foramen magnum [1].

Physicians can monitor pressure buildup by drilling a hole through the skull and draining excess fluid or placing sensors (such as the Camino monitor) inside the skull for pressure monitoring [2]. Typically a skilled neurosurgeon or a trained mid-level practitioner is required to make the hole in the skull due to the risk in damaging delicate brain tissue under the dura. Without proper training, a clinician may inadvertently advance the spinning drill bit beyond the underside of the skull by several millimeters and into brain tissue [3]. This is called "plunging" and can lead to permanent brain damage [4]. Clinicians treating TBI must develop the skills to detect drill bit penetration without plunging despite highly variable skull thickness because different areas of the skull range in thickness from 3mm to over 10mm with mean thickness 5-7mm [5]. As shown in Fig. 1, even for one patient the skull thickness could vary by several millimeters over the span of a small space.

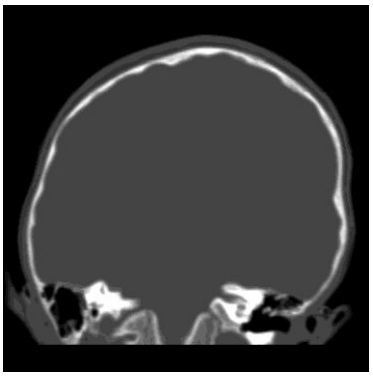

Figure 1. CT SCAN OF A PATIENT SKULL SHOWN IN WHITE [6]

Studies show that 1.4 million Americans per year suffer from some kind of head injury, totaling $76.5 billion in costs annually [7]. 275,000 of those injured are hospitalized and 52,000 will eventually die as a result of that injury [7]. Treatment of TBI is certainly worthwhile, as a study comparing the long-term effects of TBI patients with and without aggressive monitoring showed that aggressive treatment was associated with a 12% decrease in the mortality rate [8]. However, despite the thousands of people suffering from head injury, only a small percent of patients receive intracranial pressure (ICP) monitoring. This percentage is low because a skilled clinician is required to penetrate the skull and install the monitor. If safe skull penetration devices were available to a wider range of clinicians then it is possible that more patients suffering from head injury would receive and benefit from ICP monitoring [6].

Figure 2. INTEGRA CRANIAL ACCESS KIT MANUAL DRILL [9]

Currently, there are several products on the market for cranial drilling and preferences vary by institution. A frequently used manual cranial drill, part of the Integra Cranial Access Kit in Fig. 2, features a manually adjusted stopper that is set to the estimated bone thickness to prevent plunging [9]. This drill is a single-use device that is manually driven. Clinicians using this hand-cranked drill must use significant upper body strength. They frequently lean their weight into the drill (as in Fig. 3), adding pressure to the patient's head, making careful retraction difficult. Other clinicians prefer motorized drilling and use a standard electric drill along with years of training to avoid plunging.

Figure 3. CLINICIAN LEANING AGAINST MANUAL DRILL

An existing drilling device with an automatic safety stop, pictured in Fig. 4, is called a "cranial perforator." These tools feature a safety mechanism that stops drilling after skull penetration and reduces the likelihood of plunging [10]. This device uses a clutching mechanism that can engage concentric drill bits to counter-bore a large burr hole into the skull. Upon penetration, the inner drill bit is sprung forward a small amount into the cranial cavity to de-clutch the mechanism and stop the outer bit rotation. Cranial perforators remove additional bone material during the counter-boring process. The clutch mechanism cannot be scaled down to small hole sizes that are ideal for pressure monitoring and many TBI treatments. Their large bit sizes, which require high torque drills, are used in conjunction with bulky operating room equipment (e.g. pneumatic drills, air hoses, and compressors).

Figure 4. ACRA-CUT, CRANIAL PERFORATOR [10]

As numerous researchers are also interested in cranial drilling, other methods of safe drilling have been created. Robotic approaches typically feature high-tech, precise control systems while sacrificing portability and simplicity [11, 12]. These systems sense changes in electrical current or position measurements to detect when to stop drilling. Using pre-operative imaging data in conjunction with current drilling motion to detect penetration is another technique for achieving accuracy in safely drilling to a known depth [13]. However, while these techniques may be useful for accurate cranial drilling, there are many situations in which precise skull

thickness data is not available. Existing cranial drilling methods in the research lab were not designed for portability or cost effectiveness.

This paper describes the design and development of a handheld, portable, assured safety drilling prototype that can be used with any diameter drill bit to create holes in the skull without endangering underlying brain tissue. The following sections explain the functional requirements of the drill, design specifications, and mechanism modeling. The retraction model will be used to design a prototype that will be validated through ex-vivo bone drilling experiments. The assured safety drill, developed through close collaborations between engineers and clinicians, will enable a range of clinicians to safely drill holes for TBI treatment in many settings.

DESIGN PROCESS

A survey of existing cranial drilling options and meetings with clinicians emphasized the following functional requirements of the assured safety drill:

1. Handheld: Intended for use in the emergency room, disaster relief, or military settings
2. Cordless: To avoid traffic hazards and ensure mobility of clinician
3. Portable: Requires manageable size, weight
4. Variable hole size: Based on clinician's needs for various treatments
5. Inexpensive: Should cost a similar amount as current manually powered drills
6. Disposable: For convenience in field use where sterilization is not available
7. Safe: Must penetrate the skull of unknown thickness and avoid plunging

The primary difficulty in drill design is related to the safety requirement of penetrating a skull of unknown thickness. Various sensing strategies were considered to predetermine the bone depth at a desired position and then drill through to that depth exactly. Another strategy considered was to sample sensors at a high rate and cause the drill to stop spinning based on force or impedance control. Since these methods would increase complexity, be extremely reliant on sensors, could reduce portability, and likely involve an expensive combination of electrical and mechanical parts, it was ultimately decided that the safety mechanism should be as simple and robust as possible by being purely mechanical. The simplest retraction mechanism must be able to sense the change in drilling force that occurs upon penetration. It was thought that the sharp change in force could be used to trigger a bi-stable mechanism, thereby retracting the drill bit at the right time to avoid plunging.

The stages of the bi-stable mechanism are shown in Fig. 5. This mechanism was designed to be a coupler that has the drill bit on one end and can be connected on the other end to any drill of minimum spinning speed. The device uses a linkage as a bi-stable mechanism where one position supports drilling and a change in the force balance upon skull penetration causes the linkage to change positions and retract the drill bit. The initial position in Fig. 5(a) supports drilling when the links are directed towards the centerline. In Fig. 5(b) the clinician presses the drill against the patient's skull and begins drilling. Rotating masses on the linkage gather centrifugal acceleration in the radial direction while high forces in the axial direction cause the linkage to stay in the drilling position. The reduction in axial forces upon skull penetration allows centrifugal acceleration to distance the weights from the centerline, changing the linkage configuration. The linkage collapses as in Figs. 5(c)-(e) and the drill bit is quickly retracted into a plastic casing to eliminate the possibility of plunging. This configuration change is designed to occur with sufficient speed so as to retract the bit before it would come in contact with brain tissue.

Early on in the design process, a first-generation sketch model of this mechanism, shown in Fig. 6, was fabricated from low-resolution 3D printed parts and scrap materials to be a

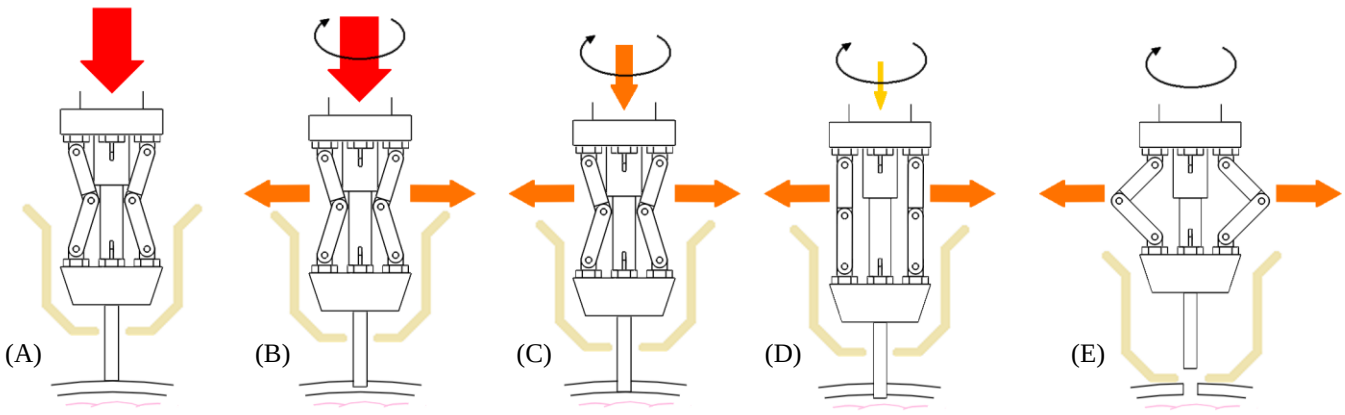

Figure 5. (A) CLINICIAN APPLIES FORCE TO DRILL, (B) SPINNING CREATES CENTRIFUGAL ACCELERATION, (C) AXIAL FORCES DECREASE AS SKULL IS PENETRATED, (D) LINKAGE BEGINS TO CHANGE CONFIGURATIONS, (E) LINKAGE COLLAPSES AND DRILL BIT IS RETRACTED

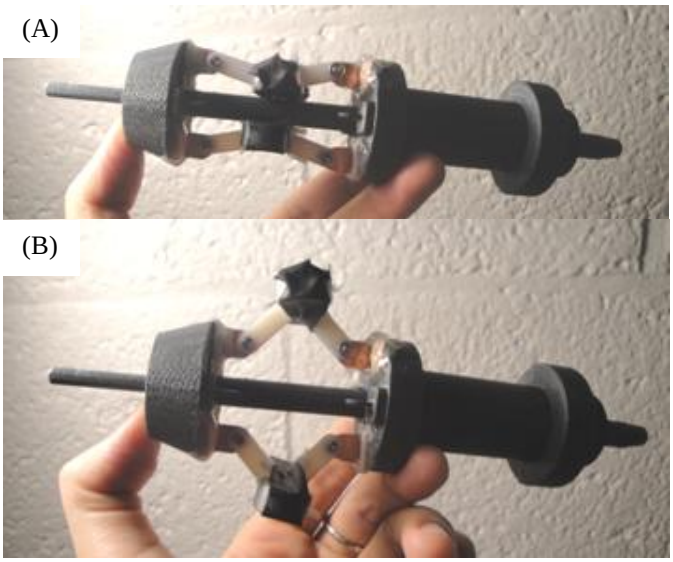

Figure 6. (A) DRILLING POSITION, (B) RETRACTED POSITION

simple proof of concept. The model was connected to a standard hardware store drill. Spinning the device showed that the linkages remained in the drilling position while force was being applied to the tip. The linkages swiftly opened when the force was removed, demonstrating the mechanism's feasibility.

MODELING OF BI-STABLE MECHANISM

An analytical model was developed to describe the behavior of the mechanism. The model was then used to select design parameters for the device prototype.

Force Balance Analysis

As shown in Fig. 7 the forces acting on the system consist of several components when the drill is vertically oriented downward towards the skull. F_{hand} is the force applied by the clinician's hand, F_g is the gravitational force of the drill, F_M is the centrifugal force due to the spinning masses, and F_{skull} is the reaction force from the skull being drilled. The force balance equation in the vertical direction is given by Eqn. (1). Equation (2) shows the centrifugal force based on m_0, the mass of the weights, ω, the spinning speed of the drill, and r, the distance from the mass to the rotational axis of the drill.

$$F_{hand} + F_g = F_{skull} \tag{1}$$

$$F_M = m_0\omega^2 r \tag{2}$$

Figure 8 shows the forces on one linkage of the device (Points A-B-C). It is assumed that the local forces acting on both linkages are equal due to symmetry. The vertical force applied to point C (F_{cy}) of each linkage is given by Eqn. (3), which is half of the summation of the reaction force from the skull, F_{skull}, the compressive force of the spring, F_{spring}, and the gravitational force of the chuck, $M_{chuck}g$. The spring, not shown in Fig. 6, is designed to connect points A and C and apply a small constant force such that the retracted drill bit does not release itself after retraction. The vertical force balance for the linkage is given by Eqn. (4). The horizontal force balance for the linkage is given by Eqn. (5).

$$F_{cy} = (F_{skull} + F_{spring} - M_{chuck}g)/2 \tag{3}$$

$$F_{ay} = F_{cy} - m_0 g \tag{4}$$

$$F_{cx} + F_{ax} = F_M + F_{bx} \tag{5}$$

Next, the moment balance for link A-B is calculated. The torque caused by F_{ax} and F_{ay} with respect to point B should balance each other, resulting in Eqn. (6), where θ is the angle between one link and the shaft (see Fig. 9). Similarly, the moment balance for link B-C with respect to point B is given by Eqn. (7).

$$F_{ax} l\cos\theta = F_{ay} l\sin\theta \tag{6}$$

$$F_{cx} l\cos\theta = F_{cy} l\sin\theta \tag{7}$$

Equations (1)-(7) can be combined and arranged to solve for F_{bx} as in Eqn. (8).

$$F_{bx} = \left(F_{skull} + F_{spring} - (M_{chuck} + m_0)g\right)\tan\theta - m_0\omega^2 r \tag{8}$$

The sign of F_{bx} has significant physical meaning. Positive F_{bx} indicates that the linkage at point B is applying force toward the centerline. The device remains in the drilling position. Negative F_{bx} indicates that force is exerted on point B away from the centerline. The motion of point B away from the

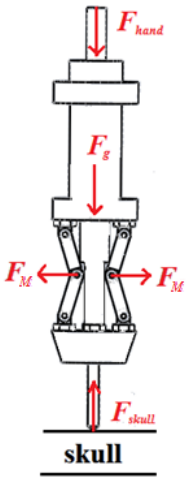

Figure 7. EXTERNAL FORCE DIAGRAM

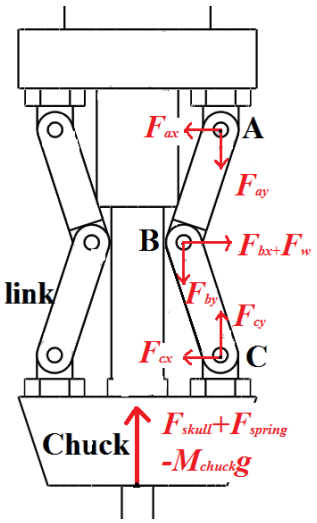

Figure 8. FORCE DIAGRAM OF ONE LINKAGE

centerline causes the linkage to change configurations and collapse.

The next step is to determine the relationship between F_{skull} and the configuration of the linkage. Plug in positive F_{bx} to Eqn. (8) and solve for F_{skull}, where F_{cr} is the critical force defined by Eqn. (9).

$$F_{skull} > m_0\omega^2 r\frac{1}{tan\theta} + (M_{chuck} + m_0)g - F_{spring} \equiv F_{cr} \quad (9)$$

If Eqn. (9) is true and F_{skull} exceeds F_{cr} the linkage will be kept in the drilling position. If Eqn. (9) is not satisfied (if $F_{skull} < F_{cr}$) then the linkage will collapse into the retracted position. Equation (9) requires the force from the clinician to the drill to be maintained during the drilling process to ensure that the linkage does not retract before drilling is finished. If the linkage does retract prematurely the clinician can easily reload the mechanism and continue drilling the same hole. Upon skull penetration the reaction force of the skull will reduce significantly [14], such that $F_{skull} < F_{cr}$. This change will cause the linkage to retract the drill bit.

Dynamic Analysis

The next stage of analysis examines the dynamics of the system to ensure that the drill bit will retract with sufficient speed to avoid plunging. The drill bit will penetrate slightly beyond the skull and it is important to minimize this total penetration distance, L_{push}, as much as possible.

Figure 9(a) shows the linkage in drilling position at the moment of skull penetration. Figure 9(b) shows the linkage in its parallel state as the bi-stable mechanism changes from drilling position towards the retracted position. Upon skull penetration the axial force F_{skull} effectively reduces to zero, the linkage becomes dynamic, and a net horizontal force, F_{out}, is applied to the mass attached to point B. Equations (10) and (11) calculate the net force and acceleration of point B.

$$F_{out} = m_0\omega^2 r + \left[(M_{chuck} + m_0)g - F_{spring}\right]tan\theta \quad (10)$$

$$a_{out} = \frac{F_{out}}{m_0} \quad (11)$$

While point B moves to the right and the linkage approaches the parallel position in Fig. 9(b), the horizontal distance that point B travels, l_{pop}, is calculated by Eqn. (12). The time to travel this distance is calculated in Eqn. (13).

$$l_{pop} = lsin\theta \quad (12)$$

$$\Delta t = \sqrt{\frac{2l_{pop}}{a_{out}}} \quad (13)$$

Assuming that the clinician will not have time to sense penetration and react on the time scale required for safe retraction, it can be assumed that the drill will vertically accelerate forward during time Δt. This vertical acceleration is

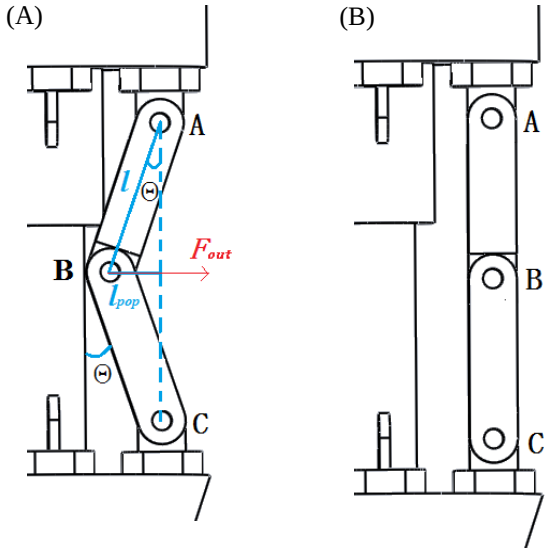

Figure 9. GEOMETRY OF LINKAGE IN (A) DRILLING POSITION, (B) PARALLEL POSITION

calculated by Eqn. (14) where M_{total} contains the masses of the drill and the assured safety device.

$$a_{push} = \frac{F_{skull}}{M_{total}} \quad (14)$$

The maximum penetration distance is calculated by summing the distance traversed by the entire drill during linkage collapse, L_1, and the protrusion of the linkage during the configuration switch, L_2. Eqns. (11)-(14) can be combined to calculate L_1 in Eqn. (15). The linkage protrusion, L_2, occurs during the configuration change as the linkage straightens in Fig. 9(b). This is calculated by Eqn. (16) and combined with Eqn. (15) to calculate L_{push} in Eqn. (17).

$$L_1 = \frac{1}{2}a_{push}\Delta t^2 = \frac{F_{skull}}{F_{out}}\frac{m_0}{M_{total}}lsin\theta \quad (15)$$

$$L_2 = 2l(1 - cos\theta) \quad (16)$$

$$L_{push} = L_1 + L_2 \quad (17)$$

$$L_{push} = l\left[\frac{F_{react} - F_{remain}}{F_{out}}\frac{m_0}{M_{total}}sin\theta + 2(1 - cos\theta)\right]$$

Selecting Design Parameters

The analysis presented above will be used to select the final design parameters for prototype construction. These factors must be considered in order to design a drill that meets functional design requirements for safety and ease of use. The chosen design parameters for a proof of concept analysis were selected from this approach.

Retraction distance. The retraction distance, L_{back}, is traversed by the drill bit upon skull penetration as the linkages collapse. This is calculated by Eqn. (18) where α is the angle between the link and the shaft in the fully open position. After the configuration change the entire drill bit should be fully retracted from the skull and encased in the housing. Therefore L_{back} must be larger than the average thickest part of the skull.

$$L_{back} = 2l(cos\theta - cos\alpha) \tag{18}$$

$$L_{back} > 10mm \tag{19}$$

Penetration Distance. To ensure that the drill bit does not damage brain tissue after penetrating the skull, the maximum penetration distance L_{push} should be limited. Neurosurgical expertise has determined that this value should never exceed 2 mm [3, 6].

$$L_{push} < 2mm \tag{20}$$

Critical Force. The critical force, F_{cr}, was calculated in Eqn. 9 as the lower limit of F_{skull} in the drilling position. Below F_{cr} the linkage will retract. Therefore F_{cr} must be designed as the lower limit of clinicians' average range of drilling forces so that the device continues drilling within the comfortable range for doctors to operate. Depending on the size of the drill bit, the feed rate, and the application, typical clinician force against the drill is expected to range from 10N to 40N [15]. This system was designed to function correctly within this broad approximate range of applied forces.

$$F_{cr} \leq 10N \tag{21}$$

Table I contains the chosen set of design parameters that can satisfy Eqns. (19)-(21). These parameters were used to build the final prototype, which will be discussed in the next section. It should be noted that the minimum required spinning speed for bit retraction is 500 rpm, but the prototype described here was designed for 1400 rpm.

Table I. DESIGN PARAMETERS

M_{total}	2.5 kg	L_{back}	11.6 mm
M_{chuck}	60 g	L_{push}	0.64 mm
m_0	10 g	F_{cr}	10.2 N
θ	10^o	F_{skull}	50 N
α	60^o	F_{spring}	10 N
R	16 mm	ω	1400 rpm
l	12 mm		

Sensitivity Analysis

It is important to determine which design parameters have the most significant effects on performance and safety. Table II was created by changing each of the parameters listed by $\pm$ 1% and calculating the resulting changes in L_{push}. Increasing θ, l, and F_{spring} or decreasing r, ω, and m_0 cause the maximum penetration distance to increase. It is evident that L_{push} is most sensitive to θ and ω. Therefore, accuracy is important in manufacturing the components which create θ. The drill must also maintain or exceed its designated spinning speed to ensure that the experimentally measured L_{push} does not exceed 2 mm.

Table II. SENSITIVITY ANALYSIS

ERROR OF L_{PUSH} DUE TO $\pm$ 1% CHANGE			
θ	$\pm$ 1.97%	r	$\mp$ 0.86%
ω	$\mp$ 1.72%	F_{spring}	$\pm$ 0.44%
l	$\pm$ 1.01%	m_0	$\mp$ 0.4%

PROTOTYPE DESIGN AND FABRICATION

The detailed design of the bi-stable mechanism was created based on the analysis in the previous section and the parameters in Table I. A number of iterations in the mechanical design optimized the component layout and improved robust connections among key moving parts in order to make the drill more compact and easier to manufacture and assemble. The long length of the device was reduced as much as possible, thereby improving the reliability of retraction and stability. The links were designed to rotate on steel pins that were easily press fitted into plastic parts. Many parts were resized to make the device as compact as possible without sacrificing material strength and the total number of parts was minimized to reduce manufacturing costs. The links were sized to retract the drill bit by 11 mm, which was the clinician-recommended distance.

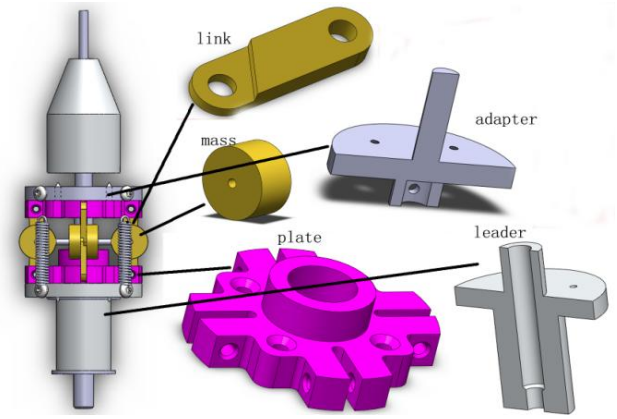

Figure 10. 3D RENDERINGS OF KEY COMPONENTS

The key components of the first prototype are pictured in Fig. 10. Several sets of masses with a variety of weights were manufactured for evaluating the sensitivity of the retraction mechanism given different work conditions (such as spinning speed, bit size, etc.). The masses were mounted on threaded pins to easily be changed between drilling tests in case different size masses were desired. The adapter, screwed into the

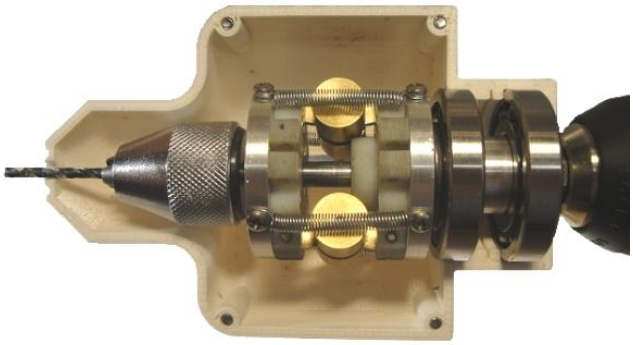

Figure 11. ASSURED SAFETY DRILLING MECHANISM PROTOTYPE

adjustable chuck, connected to the retraction shaft by a key and a pin. The plates (highlighted in pink) were mounted to the adapter and the leader. These plates had grooves containing pins on which the links rotated. The plate that attached to the leader also ensured that the proper θ was achieved by the linkage. Four springs connected the adapter and the leader for system stability as well as preventing the retracted drill bit from falling back into the skull. The leader had a long, keyed cylindrical hole through its center allowing the keyed shaft inside to slide smoothly while conveying maximum torque to the drill bit. The bottom end of the leader was designed to be fastened into the chuck of any electric-powered hand drill that meets the minimum requirements for torque and speed.

The most critical parts (links, masses, threaded pins, adapter, and leader) were machined. The links and masses were machined from brass to take advantage of the material's high density and increased centrifugal acceleration during rotation. The adapter and leader were machined from aluminum. The plates, casing, and reloading system were printed in a 3D printer for prototyping and could be made of injection molded plastics in future production. All other parts (steel pins, springs, screws, etc.) were purchased off the shelf. The prototype is pictured in Fig. 11.

EXPERIMENTAL TESTING

To evaluate the device operation a high speed camera was used to capture the drilling process with particular focus on drill bit penetration. The experimental setting is pictured in Fig. 12(a) with various bone samples. The high speed camera (with video frame rates ranging from 240-480 fps) was focused on bovine bones that were obtained from a local store. The bone samples which ranged in thickness from 5-10 mm (with layers of cortical, trabecular, and cortical bone) provided a good approximation of the human skull for these bench level experiments. Select frames from the high speed camera showed the maximum drill bit penetration in each test. An example of one such frame is shown in Fig. 12(b).

Max drill bit penetration distances were measured digitally across 39 tests and plotted in Fig. 13. The average penetration distance was 1.22 mm. The difference between the expected

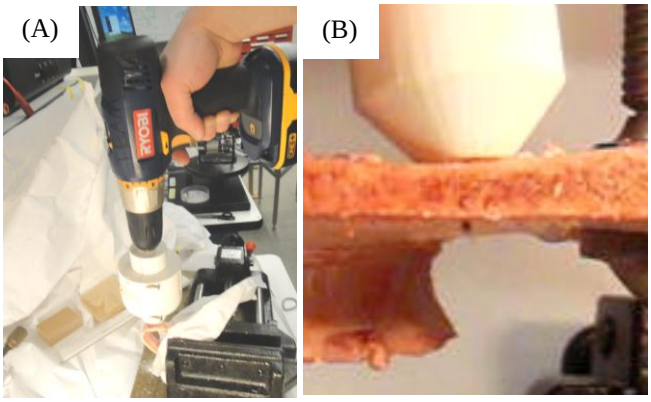

Figure 12. (A) EXPERIMENTAL SETUP WITH VARIOUS BONE SAMPLES, (B) SELECTED FRAME SHOWING MAX DRILL BIT PENETRATION

distance and the experimental results can be accounted for by manufacturing errors, unmodeled friction forces, and small changes needed in the mechanical design. While some test results showed unwanted penetration at or beyond the recommended 2 mm, preliminary results demonstrating the device's potential were highly encouraging. It should also be noted that some trials, not accounted for in Fig. 13, suffered from device failure due to looseness in screws or other parts.

CONCLUSIONS AND FUTURE WORK

This paper presented the design, fabrication, and testing of an assured safety cranial drill with an automatically retracting bit that avoids the risk of plunging after skull penetration. The drill is based on a bi-stable mechanism that is triggered by centrifugal forces to collapse the linkage at the end of penetration when the reaction force on the drill bit reduces significantly. This safe drill will decrease the experience required for safely drilling holes in the skull, enabling a wider range of clinicians to treat TBI. In particular, the availability of

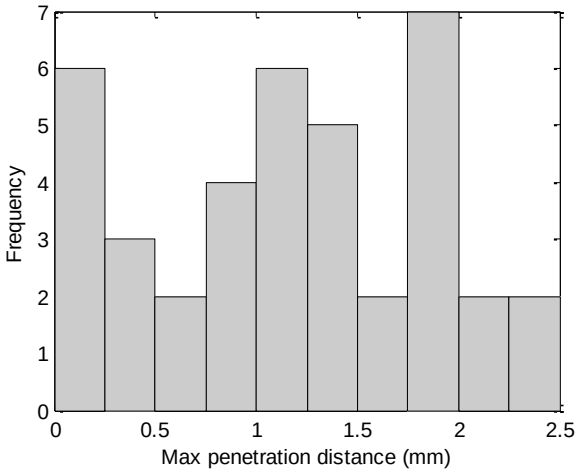

Figure 13. EXPERIMENTAL BONE DRILLING RESULTS

this device could greatly increase the frequency of ICP monitoring for TBI, reducing the negative long-term effects caused by brain trauma. Furthermore, the highly portable nature of the mechanism allows it to be used in all conditions including emergency rooms, disaster relief areas, and military operations. The drill works well in any orientation and is robust against jamming due to the mechanism's encasement. The device can be used as an attachment to an existing drill or built into a sterile, standalone portable unit. It supports drill bit diameters from 2 mm to 7 mm, covering the entire range of hole sizes needed for ICP monitoring, and could easily be fitted for larger bits if needed. Beyond cranial applications, this device could also be applied to spinal surgery, orthopedics, sternotomies, or any other surgical procedure in which a clinician wishes to drill through bone without damaging soft tissue.

Valuable experience gained in this first set of experiments can be used to greatly improve future prototypes. A set of controlled experiments will be conducted to measure the range of forces acting in this specific cranial drilling system. This information can then be applied to the model to make adjustments to the design for operating in the most optimal range of drilling forces. The friction effects in each pin joint of the current mechanism will be examined for possible material changes or machine tolerance adjustments. Additionally, other linkage configurations could increase robustness and decrease device size while reducing costs. A future prototype will use torsional springs to act on the linkage such that the natural resting state of the device is in the retracted position. The safety and efficacy of future prototypes will be verified through animal experiments.

ACKNOWLEDGMENTS

This device was developed as a project for ES227, a course at the Harvard School of Engineering and Applied Sciences taught by Professor Conor Walsh. We thank the SEAS Teaching Labs and Stan Cotreau for their guidance during the project. The authors would also like to acknowledge the Center for Integration of Medicine and Innovative Technology, the Wyss Institute for Biologically Inspired Engineering, the National Collegiate Inventors and Innovators Alliance, and Beth Israel Deaconess Medical Center for their support.

REFERENCES

[1] Agamanolis, D., Neuropathology online course, Northeastern Ohio Universities College of Medicine (NEOUCOM) http://neuropathology.neoucom.edu/chapter4/chapter4aSubdural epidural.html.

[2] Gelabert-Gonzalez, M., Ginesta-Galan, V., Sernamito-Garcia, R., Allut, A. G., Bandin-Dieguez, J., and Rumbo, R. M., 2005, "The Camino intracranial pressure device in clinical practice. Assessment in a 1000 cases," ActaNeurochirurgica, **148**, pp. 435-441.

[3] Glauser, D., Flury, P., Villotte, N., and Burckhardt, C. W., 1991, "Conception of a robot dedicated to neurosurgical operations," *Fifth International Conference on Advanced Robotics. Robots in Unstructured Environment*, **1**, pp. 899-904.

[4] Caird, J. D. and Choudhari, K. A., 2001, "'Plunging' during burr hole craniostomy: a persistent problem amongst neurosurgeons in Britain and Ireland," British Journal of Neurosurgery, **17**(6), pp. 509-512.

[5] Lynnerup, N., 2001, "Cranial thickness in relation to age, sex and general body build in a Danish forensic sample," Forensic Science International, **117**, pp. 45-51.

[6] Thomas, A.J., 2011, personal communication.

[7] Faul, M., Xu, L., Wald, M. M., and Coronado, V. G., 2010, *Traumatic Brain Injury in the United States: Emergency Department Visits, Hospitalizations and Deaths 2002–2006*, Atlanta (GA): Centers for Disease Control and Prevention, National Center for Injury Prevention and Control.

[8] Stein, S. C., Georgoff, P., Meghan, S., Mirza, K. L., and El Falaky, O. M., 2010, "Relationship of aggressive monitoring and treatment to improved outcomes in severe traumatic brain injury," Journal of Neurosurgery, **112**, pp. 1105-1112.

[9] Integra Website, Products for Neurosurgeons, Cranial Access Kit. On the WWW, Dec. 2012. URL http://integralife.com/Neurosurgeon/Neurosurgeon-Product-Detail.aspx?Product=53&ProductName=Cranial%20Access%20Kit&ProductLineName=Cranial%20Access&ProductLineID=13

[10] "Acra-Cut Smart Drill," ACRA-CUT. On the WWW, Dec. 2012. URL http://www.acracut.com/images/pdf/smartdrill.pdf

[11] Louredo, M., Diaz, I., and Gil, J. J., 2012, "DRIBON: A mechatronic bone drilling tool," Mechatronics, **22**, pp. 1060-1066.

[12] Hsu, Y.-L., Lee, S.-T., Lin, H.-W., 2011, "A modular mechatronic system for automatic bone drilling," Biomedical Engineering, Applications, Basis and Communications, **13**(4).

[13] Korff, A., Follmann, A., Fürtjes, T., Habor, D., Kunze, S. C., Schmieder, K., and Radermacher, K., 2011, "Concept and evaluation of a synergistic controlled robotic instrument for trepanation in neurosurgery," *Proc. of the IEEE Int. Conf. on Robotics and Automation (ICRA 2011)*, pp. 6258-6263.

[14] Tsai, M. D., Hsieh, M. S., Tsai, C. H., 2007, "Bone drilling haptic interaction for orthopedic surgical simulator," Computers in Biology and Medicine, **37**, pp. 1709-1718.

[15] Ong, F. R., Bouazza-Marouf, K., 1999, "The detection of drill bit break-through for the enhancement of safety in mechatronic assisted orthopedic drilling," Mechatronics, **9**, pp. 565-588.

